

# Transitions between Phases with Equal Wave Numbers in a Double Ising Spin Model. Application to Betaine Calcium Chloride Dihydrate

Boris Neubert<sup>†</sup>, Michel Pleimling<sup>‡</sup> and Rolf Siems<sup>†</sup>

<sup>†</sup>Theoretische Physik, Universität des Saarlandes, Pf. 151150, D-66041 Saarbrücken,  
e-mail: neubert@lusi.uni-sb.de

<sup>‡</sup>Theoretische Physik, Rheinisch-Westfälische Technische Hochschule, Sommerfeld-  
straße, D-52074 Aachen, e-mail: pleim@physik.rwth-aachen.de

**Abstract.** A Double Ising Spin model for uniaxially structurally modulated materials exhibits as a special feature phase transitions between phases with equal wave numbers but different pseudo spin configurations. The character of these ‘internal’ transitions is investigated in mean field approximation, with the mean field transfer matrix method, and in Monte Carlo simulations. The structural changes at the transitions are characterized by different strengths of harmonics in a Fourier analysis of the spatial modulation. A dielectric anomaly in the phase diagram of betaine calcium chloride dihydrate (BCCD) and seemingly contradictory structure analyses are explained.

PACS numbers: 64.60.Cn, 64.70.Rh, 75.10.Hk

Short title: Transitions between Phases with Equal Wave Numbers

December 4, 2017

## 1. Introduction

Materials exhibiting commensurately and incommensurately structurally modulated phases were extensively investigated during the last years. BCCD,  $(\text{CH}_3)_3\text{NCH}_2\text{COO} \cdot \text{CaCl}_2 \cdot \text{H}_2\text{O}$ , is an outstanding example: it shows a rich variety of phases, and exhibits many intricate phenomena in its phase diagram, such as indications for accumulation points of structure branchings, and the so-called dielectric  $T_S$ -anomaly [1]. The problem of the modulation and its temperature-dependence still poses many open questions. The plenitude of experimental results led to a continuing theoretical interest, and many different models for their explanation have been developed (for reviews see references [2, 3]).

We recently used the concept of symmetry-adapted local modes [4] to derive the Double Ising Spin (DIS) model [5, 6] as a symmetry-based pseudo spin model with two two-component pseudo spin variables per crystallographic unit cell: the symmetry-breaking atomic displacements occurring at the transition from the high-temperature (high-symmetry) para phase to the modulated phases at lower temperatures are expanded in terms of an appropriately chosen basis set, and the pseudo spin components  $\tau$  and  $\sigma$  are the signs of the relevant coordinates [7, 8]. In the case of materials with high-temperature phase space group  $Pnma$  (e.g. BCCD), this approach yields the Hamiltonian of the DIS model [5]:

$$H = K \sum_{ijk} \tau_{ijk} \tau_{ij(k+1)} + L \sum_{ijk} \sigma_{ijk} \sigma_{ij(k+1)} + \frac{M}{2} \sum_{ijk} (\sigma_{ijk} \tau_{ij(k+1)} - \tau_{ijk} \sigma_{ij(k+1)}) \\ + J \sum_{ijk} \tau_{ijk} (\tau_{(i+1)jk} + \tau_{i(j+1)k}) + J' \sum_{ijk} \sigma_{ijk} (\sigma_{(i+1)jk} + \sigma_{i(j+1)k}). \quad (1)$$

$i, j, k$  label the pseudo spin positions along the **a**, **b**, **c**-directions respectively. At  $T = 0$ , the in-layer couplings  $J < 0$ ,  $J' < 0$  lead to a ferro-ordering of the layers perpendicular to **c**. In **c**-direction, frustrations and therefore modulations arise because of the antagonistic effects of the symmetric nearest neighbour interactions  $K$  and  $L$  on the one hand and the antisymmetric interaction  $M > 0$  on the other hand. The stable structures (pseudo spin profiles) obtained from the statistical mechanics treatment of  $H$  are characterized by their wave numbers  $q$  given in units of  $2\pi/(\text{pseudo spin spacing})$ .

At  $T = 0$ , five stable phases are separated by multiphase lines in the  $K/M$ - $L/M$ -plane. Along these lines, an infinity of different phases are degenerate. We restrict ourselves to ferroelectric  $\tau$ - $\tau$ -interactions, i.e.  $K < 0$ ; the phase diagram for  $K > 0$  is obtained by exploiting the properties of  $H$ . In the following, we will consider the multiphase lines (a) and (b) separating, in the notation of reference [6], phase V (the pseudo spin structure repeats itself after four layers), from the ferroelectric phase I (all  $\tau$ - and  $\sigma$ -spins in ferro-order) and the mixed phase III ( $\tau$ -spins in ferro-,  $\sigma$ -spins in antiferro-order along **c**) respectively.

For low temperatures, all phases degenerate at line (a) (with  $K < 0$  and  $L < 0$ ) and obeying some rules have a finite stability range in the vicinity of this line [6]. – Incidentally, this also holds for the four-state chiral clock model which can be derived from the DIS model for the case  $K = L < 0$  and  $J = J' < 0$  [9].

In contrast to this, in the vicinity of line (b) (with  $K < 0$  and  $L > 0$ ) only four different phases (characterized by the wave numbers  $q = 0, \frac{1}{8}, \frac{1}{6},$  and  $\frac{1}{4}$ ) are stable at very low temperatures [6]. Other phases are created at higher temperatures by structure combination branching processes.

In the present paper, we report on a remarkable type of transitions in the DIS model for the case  $K < 0$  and  $L > 0$ : these ‘internal’ transitions occurring at certain temperatures  $T_{\text{int}}$  are characterized by a structural change in the pseudo spin arrangement which is not accompanied by a change of  $q$  and – in some cases – not even by a change of the symmetries of the profile.

The paper is organized as follows. In section 2, the pseudo spin profiles calculated in mean field approximation (MFA) are discussed. The results are substantiated in section 3 by employing the mean field transfer matrix method and Monte Carlo simulations, which prove that these transitions are no artefacts of MFA. In section 4, the internal transition in the  $q = \frac{1}{8}$ -phase of the DIS model is used to explain a dielectric anomaly in the fourfold phase of BCCD as well as seemingly contradictory experimental structure analysis results. Section 5 contains a summarizing discussion.

## 2. Mean field investigation of the internal transitions

The mean field approximation is often used for analysing the finite temperature behaviour of pseudo spin models. Starting point is the variational Hamiltonian

$$H_0 = - \sum_{ijk} \underline{\eta}_k \cdot \underline{S}_{ijk} \quad (2)$$

for systems with a modulation in (001)-direction, with  $\underline{S}_{ijk} = (\tau_{ijk}, \sigma_{ijk})$ . The product  $\underline{\eta}_k \cdot \underline{S}_{ijk}$  describes the interaction of the spin  $\underline{S}_{ijk}$  (which in our case has two components) with a site-dependent mean field  $\underline{\eta}_k$  depending on the averages of the neighbouring spins. The mean values  $t_\ell = \langle \tau_{ij\ell} \rangle$  and  $s_\ell = \langle \sigma_{ij\ell} \rangle$  of the pseudo spins  $\tau$  and  $\sigma$  in the layer  $\ell$  are determined by the MFA equilibrium equations ( $\beta = \frac{1}{k_B T}$ ):

$$\begin{aligned} t_\ell &= \tanh(\beta \eta_{1,\ell}), \\ s_\ell &= \tanh(\beta \eta_{2,\ell}), \end{aligned} \quad (3)$$

with the mean fields

$$\begin{aligned} \eta_{1,\ell} &= -4Jt_\ell - K(t_{\ell+1} + t_{\ell-1}) + \frac{M}{2}(s_{\ell+1} - s_{\ell-1}), \\ \eta_{2,\ell} &= -4J's_\ell - L(s_{\ell+1} + s_{\ell-1}) - \frac{M}{2}(t_{\ell+1} - t_{\ell-1}). \end{aligned}$$

Figure 1 shows a typical mean field phase diagram in the plane  $\lambda = 0.1$ ,  $j = j' = -0.25$ , where we have introduced the reduced interaction parameters  $\kappa = \frac{K}{M}$ ,  $\lambda = \frac{L}{M}$ ,  $j = \frac{J}{M}$ ,  $j' = \frac{J'}{M}$  and  $\kappa_- = \frac{1}{2}(\kappa - \lambda)$ ;  $\theta = \frac{k_B T}{M}$  denotes the reduced temperature. The shaded areas contain incommensurate and higher order commensurate phases. The different commensurate phases are characterized by their wave numbers. Para phase, ferro phase and modulated phases meet at the Lifshitz point (LP). At  $\theta = 0$  the considered cut through the temperature-interaction phase diagram intersects the multiphase line at the multiphase point MP.

The existence of accumulation points of structure branchings in the case  $K < 0$  and  $L > 0$  was verified [5] by formulating the mean field equilibrium equations (3) as a four-dimensional mapping and using a fixed-point technique analogous to that employed for the ANNNI model [10]. Also calculated were the self- and the interaction-energies of discommensurations.

As a consequence of the signs of the parameters  $K$ ,  $L$  and  $M$  (i.e.  $K < 0$ ,  $L > 0$ , and  $M > 0$ ), all phases degenerate at the multiphase line (b) consist of bands of two types of two-layer sequences viz.  $(\begin{smallmatrix} + & + \\ - & + \end{smallmatrix})$  and  $(\begin{smallmatrix} - & - \\ + & - \end{smallmatrix})$ , where the upper (lower) symbols represent the signs of the  $\tau$ - ( $\sigma$ -) spin. We introduce a bracketed notation  $\langle A_1 \dots A_k \rangle$  for the different phases: for example,  $\langle 23 \rangle$  denotes a repetitive pseudo spin structure consisting of a band with two  $(\begin{smallmatrix} + & + \\ - & + \end{smallmatrix})$  sequences followed by a band with three  $(\begin{smallmatrix} - & - \\ + & - \end{smallmatrix})$  sequences. The wave number for the above phase is

$$q = \frac{k}{4 \sum_{i=1}^k A_i}.$$

The equilibrium pseudo spin profiles for configurations with a fixed wave number  $q$  at a given temperature are obtained by finding the self-consistent solutions of the equations (3). This is done by starting from different initial spin configurations with the same modulation period and iterating. The respective free energies are calculated and the solution with the lowest free energy describes the stable spin configuration. Keeping  $\lambda$ ,  $j$ , and  $j'$  fixed, the reduced parameters  $\theta$  and  $\kappa_-$  are then varied in such a way that the resulting line  $\theta(\kappa_-)$  always lies wholly in the stability region of the phase under investigation. Figure 2 shows the obtained spin profiles for the phases  $\langle 12 \rangle$  (wave number  $q = \frac{1}{6}$ ) and  $\langle 2 \rangle$  ( $q = \frac{1}{8}$ ) with  $\lambda = 0.05$  and  $j = j' = -1$ . For both wave numbers there is a discontinuous internal phase transition. At higher temperatures, the  $q = \frac{1}{6}$ -phase exhibits also a continuous transition to a modification with two disordered layers.

The obtained spin profiles for the  $\langle 2 \rangle$ -phase (for layers 1 to 8, i.e. for one modulation period) exhibit symmetries given by

(a) at low temperatures:

$$\begin{array}{cccccccc} t : & t_1 & t_2 & t_2 & t_1 & -t_1 & -t_2 & -t_2 & -t_1 \\ s : & -s_1 & s_2 & -s_2 & s_1 & s_1 & -s_2 & s_2 & -s_1 \end{array}$$

(b) at high temperatures:

$$\begin{array}{cccccccc} t : & t_1 & t_2 & t_2 & t_1 & -t_1 & -t_2 & -t_2 & -t_1 \\ s : & -s_1 & -s_2 & s_2 & s_1 & s_1 & s_2 & -s_2 & -s_1. \end{array}$$

At a reduced temperature  $\theta_{\text{int}}$  the  $\sigma$ -spins averages change signs in layers 2, 3, 6 and 7, whereas the symmetry elements of the spin profiles are left unchanged. Furthermore, also the  $\tau$ -spins (in all layers) show discontinuities at  $\theta_{\text{int}}$ .

For the  $\langle 12 \rangle$ -phase, the spin profiles in the vicinity of the discontinuous transition are:

(a) at low temperatures:

$$\begin{array}{ccccccc} t & : & t_1 & t_1 & -t_2 & -t_3 & -t_3 & -t_2 \\ s & : & -s_1 & s_1 & s_2 & -s_3 & s_3 & -s_2 \end{array}$$

(b) at high temperatures:

$$\begin{array}{ccccccc} t & : & t_1 & t_2 & t_3 & -t_1 & -t_2 & -t_3 \\ s & : & -s_1 & s_2 & s_3 & s_1 & -s_2 & -s_3. \end{array}$$

In this case the  $\tau$ -spins in layer 3 (and the  $\sigma$ -spins in layers 4 and 5) change signs, leading to a change of the symmetries of the profile.

In general not all combinations of the signs of the spins were taken as possible starting points for solving the equilibrium equations self-consistently. However, we substantiated our results for selected values of the parameters by considering all  $2^{11}$  (phase  $\langle 12 \rangle$ ) or  $2^{15}$  (phase  $\langle 2 \rangle$ ) possible sign combinations (changing the signs of all spins leaves the free energy unchanged).

In order to characterize the different modifications, a Fourier analysis of the spatial modulation of  $t_\ell$  and  $s_\ell$  was performed. In the following, the results for the  $q = \frac{1}{8}$ -phase are discussed, as they will be needed for the application to BCCD in section 4. For reduced temperatures slightly below ( $\theta = 2.967$ ) and above ( $\theta = 2.993$ ) the reduced temperature  $\theta_{\text{int}}$  of the internal transition, the pseudo spin averages (profiles) for one period of the spatial modulation are shown in figure 3 together with their harmonics. Due to the symmetries in the pseudo spin profiles, the Fourier components of  $t_\ell$  ( $s_\ell$ ) are all odd (even) about  $\ell = \frac{1}{2}$ , and only odd orders in sine (cosine) occur in the Fourier series:

$$t_\ell = a_1 \sin\left(\frac{\pi}{4}\left[\ell - \frac{1}{2}\right]\right) + a_3 \sin\left(\frac{3\pi}{4}\left[\ell - \frac{1}{2}\right]\right) \quad (4)$$

$$s_\ell = b_1 \cos\left(\frac{\pi}{4}\left[\ell - \frac{1}{2}\right]\right) + b_3 \cos\left(\frac{3\pi}{4}\left[\ell - \frac{1}{2}\right]\right). \quad (5)$$

Upon cooling (see figure 4), the relative strength of the third order harmonic with respect to the first order harmonic increases smoothly from zero near the transition to the para phase to about one third near  $\theta_{\text{int}}$  (both for the  $t$ - and  $s$ -profiles). When dropping below  $\theta_{\text{int}}$ , only a slight increase in  $a_1$  and  $a_3$  but remarkable changes in  $b_1$  and  $b_3$  occur:  $b_3$  jumps from 0.391 at  $\theta = 2.993$  to  $-1.089$  at  $\theta = 2.967$  while  $|b_1|$  decreases from 1.136 to 0.536. Below  $\theta_{\text{int}}$ , the  $s$ -profile is governed by the strong third order harmonic ( $|b_3/b_1| > 2.03$ ), which continuously increases to the ground state value  $|b_3| = 1.307$ , whereas the first harmonic keeps its nearly constant value  $|b_1| = 0.54$ .

In MFA, these discontinuous internal phase transitions were obtained for all investigated phases of the DIS model, excepting only the  $\langle 1 \rangle$ - and the  $\langle \infty \rangle$ - (ferro) phases. They occur for all values of  $\lambda$  and  $\kappa$  as long as  $\lambda > 0$  and  $\kappa < 0$ , as well as for all in-layer couplings  $j$  and  $j'$  (even for very large values).

### 3. Verification by mean field transfer matrix and Monte Carlo methods

In the previous section, the DIS model was treated in the mean field approximation. The question arises whether the observed internal transitions are an artefact of this approximation or if they are also present if one goes beyond mean field theory.

This problem should indeed be considered: in MFA, the Axial Next Nearest Neighbour Ising (ANNNI) model [11] with weak in-layer couplings exhibits, for example, phase transitions from the low temperature phases to high temperature asymmetric and partially disordered phases [12]. Nakanishi [13] could show that these phases are MFA artefacts by demonstrating that they do not occur if the mean field transfer matrix (MFTM) method is used, in which the interactions in direction of the modulations are treated exactly. The same conclusion was drawn from Monte Carlo simulations [14].

In the MFTM method, the variational Hamiltonian for the DIS model is

$$H_0 = K \sum_{ijk} \tau_{ijk} \tau_{ij(k+1)} + L \sum_{ijk} \sigma_{ijk} \sigma_{ij(k+1)} + \frac{M}{2} \sum_{ijk} (\sigma_{ijk} \tau_{ij(k+1)} - \sigma_{ij(k+1)} \tau_{ijk}) - \sum_{ijk} \underline{\eta}_k \cdot \underline{S}_{ijk}. \quad (6)$$

In the MFA variational Hamiltonian (1) all interactions are described by mean fields. In contrast, in equation (6) site-dependent mean fields are only introduced for the interactions perpendicular to the direction of modulation. As the two-component mean fields  $\underline{\eta}_k$  do not depend on the indices  $i$  and  $j$  the problem is reduced to one dimension and the indices  $i$  and  $j$  will be omitted.

Using the Bogoliubov variational principle, the MFTM free energy is given by

$$F = 2J \sum_{\ell} t_{\ell}^2 + 2J' \sum_{\ell} s_{\ell}^2 + \sum_{\ell} \eta_{1,\ell} t_{\ell} + \sum_{\ell} \eta_{2,\ell} s_{\ell} - k_B T \ln Z \quad (7)$$

with

$$Z = \text{Tr} \exp \left( \tilde{K} \sum_{\ell} \tau_{\ell} \tau_{\ell+1} + \tilde{L} \sum_{\ell} \sigma_{\ell} \sigma_{\ell+1} + \frac{\tilde{M}}{2} \sum_{\ell} (\tau_{\ell+1} \sigma_{\ell} - \sigma_{\ell+1} \tau_{\ell}) + \sum_{\ell} (h_{1,\ell} \tau_{\ell} + h_{2,\ell} \sigma_{\ell}) \right) \quad (8)$$

and  $\tilde{K} = \beta K$ ,  $\tilde{L} = \beta L$ ,  $\tilde{M} = \beta M$  and  $h_{1,\ell} = \beta \eta_{1,\ell}$ ,  $h_{2,\ell} = \beta \eta_{2,\ell}$ . In order to calculate the partition function  $Z$  we introduce the transfer matrix

$$T_{\ell} = \begin{pmatrix} e^{h_{1,\ell}+h_{2,\ell}} & 0 & 0 & 0 \\ 0 & e^{h_{1,\ell}-h_{2,\ell}} & 0 & 0 \\ 0 & 0 & e^{-h_{1,\ell}+h_{2,\ell}} & 0 \\ 0 & 0 & 0 & e^{-h_{1,\ell}-h_{2,\ell}} \end{pmatrix} \begin{pmatrix} e^{\tilde{K}+\tilde{L}} & e^{\tilde{K}-\tilde{L}+\tilde{M}} & e^{-\tilde{K}+\tilde{L}-\tilde{M}} & e^{-\tilde{K}-\tilde{L}} \\ e^{\tilde{K}-\tilde{L}-\tilde{M}} & e^{\tilde{K}+\tilde{L}} & e^{-\tilde{K}-\tilde{L}} & e^{-\tilde{K}+\tilde{L}+\tilde{M}} \\ e^{-\tilde{K}+\tilde{L}+\tilde{M}} & e^{-\tilde{K}-\tilde{L}} & e^{\tilde{K}+\tilde{L}} & e^{\tilde{K}-\tilde{L}-\tilde{M}} \\ e^{-\tilde{K}-\tilde{L}} & e^{-\tilde{K}+\tilde{L}-\tilde{M}} & e^{\tilde{K}-\tilde{L}+\tilde{M}} & e^{\tilde{K}+\tilde{L}} \end{pmatrix}.$$

For a commensurate phase with period  $p$  the mean fields repeat themselves after  $p$  layers. The partition function (8) is then given by  $Z = \alpha_{max}^{N/p}$  where  $\alpha_{max}$  is the maximum eigenvalue of the matrix product  $\prod_{\ell=1}^p T_{\ell}$  and  $N$  is the number of layers in the crystal.

The mean values  $t_{\ell}$  and  $s_{\ell}$  are calculated by

$$\begin{aligned} t_{\ell} &= \frac{\partial \ln \alpha_{max}}{\partial h_{\ell}^1} = \frac{1}{\alpha_{max}} \langle \alpha_{max} | T_1 \dots T_{\ell-1} \mu^t T_{\ell} \dots T_p | \alpha_{max} \rangle \\ s_{\ell} &= \frac{\partial \ln \alpha_{max}}{\partial h_{\ell}^2} = \frac{1}{\alpha_{max}} \langle \alpha_{max} | T_1 \dots T_{\ell-1} \mu^s T_{\ell} \dots T_p | \alpha_{max} \rangle. \end{aligned} \quad (9)$$

$\langle \alpha_{max} |$  and  $| \alpha_{max} \rangle$  are the left and the right eigenvectors corresponding to the eigenvalue  $\alpha_{max}$ , whereas the matrices  $\mu^t$  and  $\mu^s$  are given by

$$\mu^t = \begin{pmatrix} 1 & 0 & 0 & 0 \\ 0 & 1 & 0 & 0 \\ 0 & 0 & -1 & 0 \\ 0 & 0 & 0 & -1 \end{pmatrix} \quad \text{and} \quad \mu^s = \begin{pmatrix} 1 & 0 & 0 & 0 \\ 0 & -1 & 0 & 0 \\ 0 & 0 & 1 & 0 \\ 0 & 0 & 0 & -1 \end{pmatrix}.$$

The mean fields

$$\eta_{1,\ell} = -4Jt_{\ell} \quad \text{and} \quad \eta_{2,\ell} = -4J's_{\ell} \quad (10)$$

result from the minimization of the free energy (7). Equations (9) and (10) are to be solved self-consistently.

As an example, we will discuss the application of this method to the  $q = \frac{1}{8}$  phase. Calculations in mean field approximation (see previous section) yield a first order phase transition at  $\theta_{\text{int}}$  between a low- and a high-temperature modification (figure 2). These two spin profiles are used as starting points for the self-consistent solution of the MFTM equations (9) and (10).

Figure 5 shows the resulting free energies obtained by varying the model parameters in the same manner as in the previous section, i.e. one proceeds along the same  $\theta(\kappa_-)$ -curve as for the MFA calculations. It is clearly seen that the free energy curves of the

two modifications intersect at  $\theta_{\text{int}} = 2.91$ , yielding a first-order phase transition. As expected, the temperature  $\theta_{\text{int}}$  is slightly shifted to lower temperatures as compared to the MFA result.

In the MFTM method some pseudo spin interactions, though not those in modulation direction (which should be the most important ones), are still replaced by an interaction of the pseudo spins with a mean field. To make sure that this approximation is not responsible for the occurrence of internal phase transitions, Monte Carlo simulations were performed for phases with a short modulation length. No attempt was made to determine the global phase diagram.

Systems of sizes  $L \times L \times M$  were simulated, with  $L$  ranging from 10 to 40. The number of layers,  $M$ , is given by the modulation length of the phase under investigation, e.g.  $M = 6$  for the  $q = \frac{1}{6}$ -phase. This is done in order to avoid the development of fluctuations resulting from (meta)stable phases with a larger modulation length. The standard one-spin-flip Metropolis algorithm is used.

Figure 6 shows the calculated specific heat as a function of the reduced temperature for the  $q = \frac{1}{6}$ -phase, for interactions given by  $\lambda = 0.1$ ,  $\kappa = -0.57$ , and  $j = j' = -0.5$  and a size of  $30 \times 30 \times 6$ . There are two different peaks. The peak at higher temperatures corresponds to a second order phase transition to the disordered phase. In the present context, the narrow peak is the interesting one. It corresponds to the internal first order phase transition. The resulting spin profiles for temperatures below and above the peak position compare favorably with the profiles obtained in MFA. In the inset showing the calculated energy the discontinuous character of the internal phase transition is clearly visible.

#### 4. Application to BCCD

Due to the pseudo symmetry of half a lattice constant along  $\mathbf{c}$ , BCCD can be considered to be built up of successive layers of half cells perpendicular to  $\mathbf{c}$ , which we label by the subscript  $\ell$ . Applying the method described in reference [7] to BCCD, the symmetry-breaking atomic displacements occurring below the transition from the unmodulated high-temperature phase to the modulated phases are expanded in terms of a localized symmetry-adapted basis set; the respective coordinates (mode amplitudes) are projected onto two-valued pseudo spin variables leading to symmetry-based pseudo spin models. Every basis vector (symmetry-adapted local mode, SALM) describes a collective displacement of all atoms in a half cell. One obtains two relevant SALMs for the front and two for the back half cell. Adequate superpositions of these describe structural modulations transforming according to the irreducible representations  $\Lambda_2$  and  $\Lambda_3$  of the group of the wave vector  $\mathbf{q} = q\mathbf{c}^*$  (antisymmetric with respect to the mirror plane).



The pseudo spins  $\tau$  and  $\sigma$  represent the signs of the amplitudes of the two relevant SALMs. For convenience, we shall henceforth call the latter ‘ $\tau$ -SALM’ and ‘ $\sigma$ -SALM’. Previously [3, 8], we deduced the displacements corresponding to the  $\tau$ - and the  $\sigma$ -SALMs for all BCCD atoms from experimental data [15]. For a complete visualization of these SALM displacements it is sufficient to follow the  $y$ -displacements of the nitrogen atoms. Consider the two nitrogen atoms 1 and 2 associated to a half cell. The major part of their  $y$ -displacements is provided by the  $\tau$ -SALM contributions (equal for 1 and 2). The  $\sigma$ -SALM contributions (of equal sizes but opposite signs for 1 and 2) account for the small relative  $y$ -displacement of 1 and 2.

Taking the transformation properties of the SALMs into account, the form (1) of the pseudo spin Hamiltonian is obtained as well as expressions for the spontaneous polarization in terms of the pseudo spins [3, 8].

Experimental investigations of the pressure-temperature ( $p$ - $T$ ) phase diagram of BCCD [16, 17, 18] revealed a dielectric anomaly in the modulated phase with wave vector  $\mathbf{k} = \frac{1}{4}\mathbf{c}^*$ . It occurs along a line  $T_S(p)$ , which runs almost parallel to the boundary of the para phase and to the lines of constant spontaneous polarization  $P_{S,x}$ . At ambient pressure,  $T_S$  practically coincides with the upper boundary of the fourfold phase. The  $T_S$ -anomaly exhibits the characteristics of a first order phase transition; it leaves the wave number unchanged. One proposal for the explanation of the  $T_S$ -anomaly was to interpret it as a freezing of the soliton lattice [18], i.e. to assume that the soliton lattice is free to move above  $T_S$  and is pinned below.

Since the wave number  $k$  in BCCD is measured in units of the reciprocal lattice constant, whereas the wave number  $q$  in the DIS model is given in units of the reciprocal layer spacing, the  $k = \frac{1}{4}$ -phase in BCCD corresponds to the  $q = \frac{1}{8}$ -phase in the DIS formalism. For the latter the occurrence of an internal transition was explicitly shown in sections 2 and 3 above. It suggests itself to interpret the  $T_S$ -anomaly as a manifestation of the internal transition observed in the DIS model. This hypothesis is supported by the following results:

In the same way as the  $T_S$ -line in BCCD, the  $T_{\text{int}}$ -line runs parallel to the boundary of the high-temperature phase and parallel to the lines of constant spontaneous polarization [3]  $P_{S,x} = \sum_{\ell} (-1)^{\ell} [P_x^1 t_{\ell} t_{\ell+1} + P_x^2 s_{\ell} s_{\ell+1} + P_x^3 s_{\ell} t_{\ell} + P_x^4 (t_{\ell} s_{\ell+1} - s_{\ell} t_{\ell+1})]$ .

There is an interesting connection with experimental studies on the structure of the fourfold phase in BCCD:

The displacement of atom  $\mu$  in cell  $\mathbf{n}$  can be written as (e.g. reference [19])

$$\mathbf{u}_{\mathbf{n}}^{\mu} = \sum_{m \geq 1} \left[ \mathbf{e}_m^{1\mu} \cos(2\pi m \mathbf{k} \cdot (\mathbf{r}_{\mathbf{n}} + \rho^{\mu})) + \mathbf{e}_m^{2\mu} \sin(2\pi m \mathbf{k} \cdot (\mathbf{r}_{\mathbf{n}} + \rho^{\mu})) \right], \quad (11)$$

where the zeroeth order harmonics are absorbed in the average positions  $\rho^{\mu}$  of  $\mu$  with respect to the origin of the cell. There are only odd harmonics due to the symmetry of the  $k = \frac{1}{4}$ -phase in BCCD. A comparison of the symmetries of the eigenvectors  $\mathbf{e}_m^{1\mu}$  and

$\mathbf{e}_m^{2\mu}$  for odd  $m$  and of the  $\tau$ -SALM and the  $\sigma$ -SALM shows that the sin and cos terms in (11) correspond to the  $t$ - and  $s$ -profile respectively [8].

Recent neutron scattering studies [19] of the fourfold phase in BCCD at 100K and ambient pressure (see figure 7a), i.e. below  $T_S \approx 115K$ , revealed a strong third harmonic in the cos terms in (11). This is in perfect agreement with the structure of the low temperature modification in the DIS model as derived in sections 2 and 3. X-ray techniques [15] showed a more sinusoidal modulation ( $T = 90K$ , ambient pressure), which can be well described as the high temperature modification in the DIS model, i.e. the one that is expected to be stable above  $T_S$ .

These seemingly contradictory experimental results can be explained if the influence of point defects on the phase diagram and recent experiments on intentionally X-ray-irradiated samples are taken into consideration. Exposure to X-rays – even to doses used normally in diffractometry [20, 17] – produces radiation damage, which is sufficient to cause an observable lattice expansion. The effect is comparable to doping with bromine ions. The resulting (positive) plastic strains shift the boundaries in the  $p$ - $T$ -phase diagram to higher pressures/lower temperatures. It was experimentally observed, that this shift is stronger for the  $T_S$ -line than for the other phase boundaries [17, 18]. This leads to the situation described schematically in figure 7b: the irradiation defects induced by the X-ray measurements produce different shifts of the  $T_S$ -line and the other boundaries and thus open up a window for the observation of the high temperature modification of the  $k = \frac{1}{4}$ -phase at ambient pressure.

For a more quantitative comparison of the structures predicted by the symmetry-based DIS model with the atomic displacements observed either by X-ray or by neutron measurements, we derived the amplitudes  $Q_\ell^\tau$  and  $Q_\ell^\sigma$  in a decomposition of the structural modulation in the fourfold phase of BCCD in terms of the  $\tau$ - and  $\sigma$ -SALMs (see figure 8) from the experimental data given in references [19, 15]. In the employed procedure [3],  $Q_\ell^\tau$  and  $Q_\ell^\sigma$  are proportional to  $t_\ell$  and  $s_\ell$  in linear approximation.  $Q_\ell^\tau$  and  $Q_\ell^\sigma$  can be written in terms of first and third order harmonics as in equations (4) and (5). We obtained  $a_3/a_1 = 0.15$ ,  $b_3/b_1 = -0.08$  from the X-ray data [15] and  $a_3/a_1 = 0.27$ ,  $b_3/b_1 = 2.35$  from the neutron results [19]. Similar values can be found in the DIS model for temperatures not too far above (e.g.  $\theta = 4.25$ :  $a_3/a_1 = 0.18$ ,  $b_3/b_1 = -0.07$ ) or below  $\theta_{\text{int}}$  (e.g.  $\theta = 2.76$ :  $a_3/a_1 = 0.39$ ,  $b_3/b_1 = 2.13$ ) respectively. It is noteworthy that even with the parameters ( $\lambda = 0.05$ ,  $j = j' = -1.0$ ) which were rather arbitrarily chosen in this comparison and which probably do not represent the optimal choice (e.g. by the methods discussed in ref. [3]) for BCCD, we find a good agreement between theoretical prediction and experimental observation.

## 5. Conclusions

Recent theoretical developments in the field of modulated systems allow, in a physically well motivated way, to bridge the gap between pseudo spin model-parameters and -properties on the one hand, and experimental control parameters and physical characteristics of real systems on the other.

An efficient pseudo spin model, which is well suited as a basis both for largely analytical calculations and for numerical simulations, is the DIS model. It can advantageously be used for the theoretical description of a large class of modulated materials. Since the model variables are explicitly related to local properties of the discrete crystal lattice, it allows explicit predictions e.g. of structures, symmetries, spontaneous polarizations, phase diagrams, and orders of transitions of modulated phases in real systems.

A special feature of the DIS model is that it predicts phase transitions not only between modulated structures with different wave numbers, but also between modulations with the same wave number but different pseudo spin configurations ('internal' phase transitions). The respective phases differ significantly in the amplitudes of the harmonics in a Fourier expansion of the pseudo spin profiles and in symmetry. Since remotely similar theoretical results derived for the ANNNI model were later shown to be artefacts of the employed mean field approximation, we verified the validity of our MFA results both by means of the mean field transfer matrix method and by Monte Carlo simulations.

One indication of the suitability of the symmetry-based DIS model for the description even of detailed characteristics of complex modulated real systems is the proposed explanation of the dielectric anomaly  $T_S$  observed in the fourfold phase of BCCD: this anomaly and its characteristic properties can be well interpreted as a realization of the internal phase transitions of the DIS model.

Furthermore, an application of the general procedure for translating model properties to characteristics of real, experimentally investigated systems allows a tentative explanation of discrepancies between experimental structure determinations of the fourfold phase of BCCD by neutrons on the one hand and by X-rays on the other. Taking the influence of X-ray induced defects (via the strain field) into account, we propose a mechanism which allows the high temperature modification of the fourfold phase (which exists in ideal crystals only at elevated pressure) to become stable already at ambient pressure and, thus, be visible in X-ray measurements. The two experimentally determined structures of the fourfold phase agree fairly well with our calculated data.

## Acknowledgments

Stimulating discussions with Prof. Dr. J.M. Pérez-Mato, Bilbao, and financial support from the Deutsche Forschungsgemeinschaft (research grant Si 358/2) are gratefully acknowledged.

## References

- [1] The status of the present experimental situation is given in Schaack G and Le Maire M 1998 *Ferroelectrics* (in press)
- [2] Blinc R and Levanyuk A P 1986, editors, *Incommensurate Phases in Dielectrics, 1. Fundamentals*. (Amsterdam: North-Holland); Selke W 1992 In: Domb C and Lebowitz J L, editors, *Phase Transitions and Critical Phenomena*, vol 15 (London: Academic Press) p 1;
- [3] Neubert B, Pleimling M and Siems R 1998 *Ferroelectrics* (in press)
- [4] Thomas H 1971 In: Samuelsen E J, Andersen E and Feder J, editors, *Structural Phase Transitions and Soft Modes*, (Oslo, Bergen, Tromsø: Universitetsforlaget) p 15
- [5] Pleimling M and Siems R 1994 *Ferroelectrics* **151** 69
- [6] Pleimling M and Siems R 1996 *Ferroelectrics* **185** 103
- [7] Neubert B, Pleimling M and Siems R 1998 *J. Kor. Phys. Soc.* **32** S36
- [8] Neubert B 1998 *Symmetriebasierte mikroskopische Modelle für modulierte Materialien*, (Saarbrücken: Pirrot)
- [9] Pleimling M, Neubert B and Siems R *Low temperature phase diagram and critical behaviour of the four-state chiral clock model*, to appear in *J. Phys. A*
- [10] Jensen M H and Bak P 1983 *Phys. Rev. B* **27** 6853; Siems R and Tentrup T 1989 *Ferroelectrics* **98** 303
- [11] Selke W 1988 *Phys. Rep.* **170** 213
- [12] Yokoi C S O 1991 *Phys. Rev. B* **43** 8487; Cadorin J L and Yokoi C S O 1993 *Brazilian Journal of Physics* **23** 382
- [13] Nakanishi K 1992 *J. Phys. Soc. Jpn.* **61** 2901
- [14] Rotthaus F and Selke W 1993 *J. Phys. Soc. Jpn.* **62** 378
- [15] Ezpeleta J M, Zúñiga F, Pérez-Mato J M, Paciorek W and Breczewski T 1992 *Acta Cryst. B* **48** 261
- [16] Schaack G, Le Maire M, Schmitt-Lewen M, Illing M, Lengel A, Manger M and Straub R 1996 *Ferroelectrics* **183** 205
- [17] Le Maire M 1996 *Einfluß von Gitterdefekten auf die modulierten Phasen von Betain-Calciumchlorid-Dihydrat* PhD thesis (Würzburg, Germany)
- [18] Le Maire M, Straub R and Schaack G 1997 *Phys. Rev. B* **56** 134
- [19] Hernandez O, Quilichini M, Cousson A, Paulus W, Kiat J-M, Goukassov A, Ezpeleta J M, Zúñiga F J, Pérez-Mato J M, Dušek M and Petříček V 1998 *Proceedings of Aperiodic 1997* (in press); Hernandez O 1997 *Étude par diffusion de neutrons du chlorure de calcium et de bétaine dihydraté sous champ externe appliqué (température, champ électrique et pression hydrostatique)*, PhD thesis (Paris, France)
- [20] Kiat J M, Calvarin G, Chaves M R, Almeida A, Klöpperpieper A and Albers J 1995 *Phys. Rev. B* **52** 798

## Figure captions

**Figure 1.** Reduced temperature-interaction phase diagram of the DIS model with  $\lambda = 0.1$  and  $j = j' = -0.25$  (see text). Shown are the paraelectric, the ferroelectric, and a few commensurate phases. Higher order commensurate and incommensurate phases are contained in the hatched areas. LP is the Lifshitz point, MP the multiphase point.  $\theta$  is the reduced temperature  $\frac{k_B T}{M}$ , whereas  $\kappa_-$  is given by  $\kappa_- = \frac{1}{2}(\kappa - \lambda)$ . The phases are characterized by quotients  $q = m/n$  giving the modulation wave numbers in units of  $2\pi/(\text{pseudo spin spacing})$ .

**Figure 2.** Pseudo spin profiles for (a) the  $\langle 12 \rangle$ -phase ( $q = \frac{1}{6}$ ) and (b) the  $\langle 2 \rangle$ -phase ( $q = \frac{1}{8}$ ) as functions of the reduced temperature  $\theta$  with  $\lambda = 0.05$  and  $j = j' = -1$ . Shown are the mean values  $t_\ell$  (solid lines) and  $s_\ell$  (dashed lines), for layers  $\ell$  from 1 to the modulation length, i.e. from 1 to 6 for case (a) and from 1 to 8 for case (b).

**Figure 3.** Pseudo spin profiles  $t_\ell$  (upper part) and  $s_\ell$  (lower part) of the  $q = \frac{1}{8}$ -phase for reduced temperatures slightly below ( $\theta = k_B T/M = 2.967$ , left hand side) and slightly above ( $\theta = 2.993$ , right hand side) the internal transition  $\theta_{int}$ . Only first (solid lines) and third (dashed lines) order harmonics in sine (cosine) are present in the Fourier expansion of  $t_\ell$  ( $s_\ell$ ).

**Figure 4.** Amplitudes of the first and third order harmonics in the pseudo spin profiles  $t_\ell$  and  $s_\ell$  of the  $q = \frac{1}{8}$ -phase as functions of the reduced temperature  $\theta = k_B T/M$  [see equations (4) and (5)]. The internal phase transition at  $\theta_{int}$  separates the low temperature modification with dominant third harmonic in  $s$  from the much less anharmonic high temperature modification.

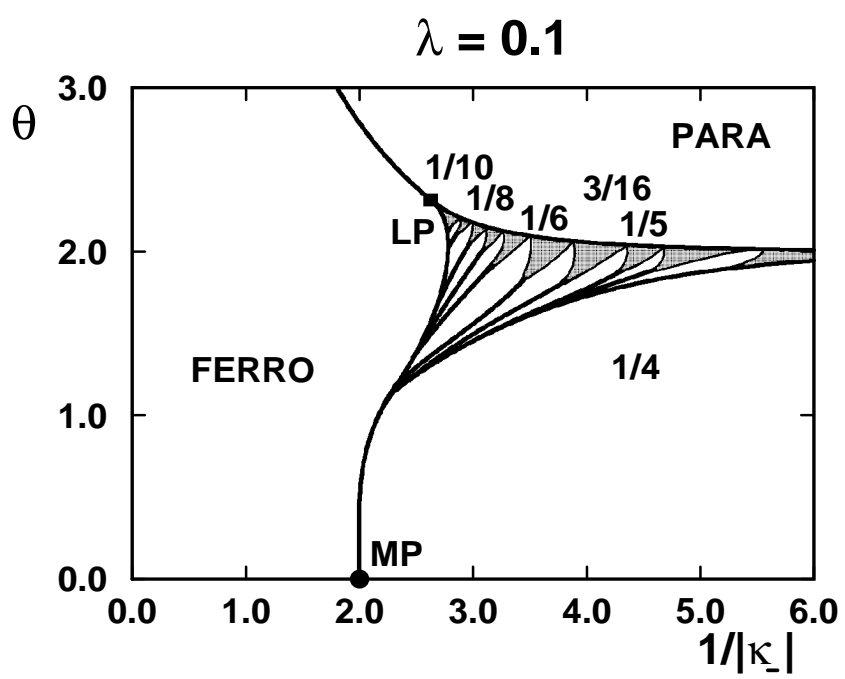
**Figure 5.** MFTM values for the reduced free energies  $F/M$  of the low- (dashed line) and the high-temperature (solid line) modifications of the  $q = \frac{1}{8}$  phase as function of the reduced temperature  $\theta$ . Fixed parameters are  $\lambda = 0.05$  and  $j = j' = -1$ . Solid line: low temperature modification; dashed line: high temperature modification. For better clarity,  $F/M - \theta + 4$  is plotted.

**Figure 6.** Specific heat of the  $q = \frac{1}{6}$ -phase obtained from Monte Carlo simulations of DIS systems with  $30 \times 30 \times 6$  spin sites.  $\lambda = 0.1$ ,  $\kappa = -0.57$ , and  $j = j' = -0.5$ . The inset shows the calculated reduced energy as a function of  $\theta$ .

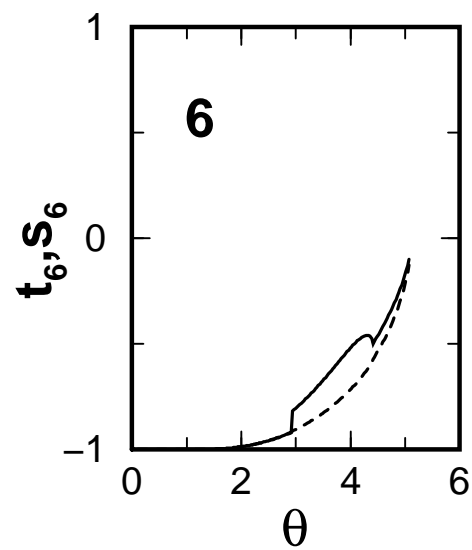
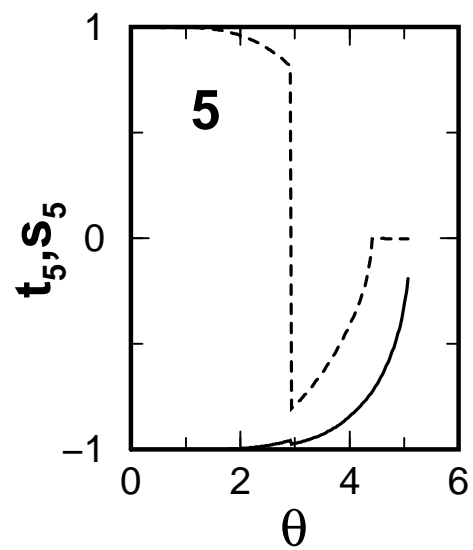
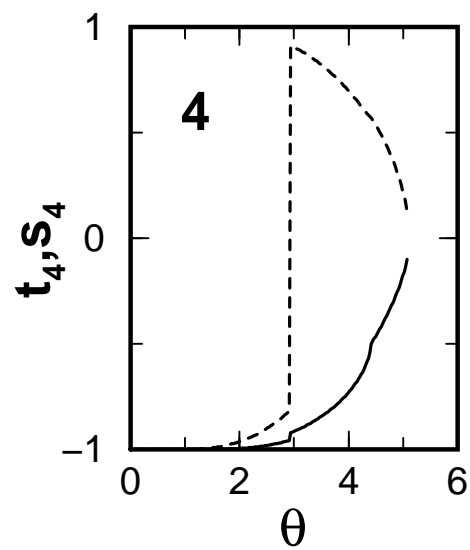
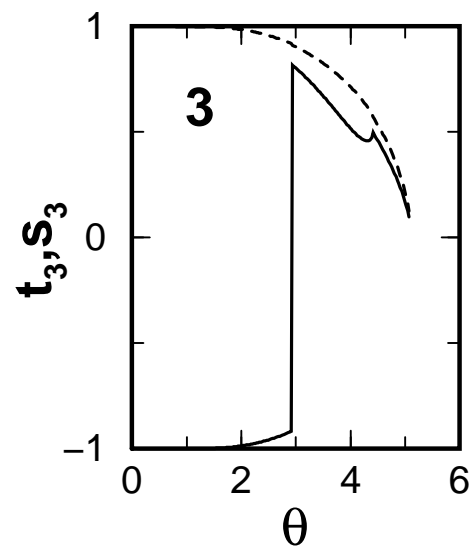
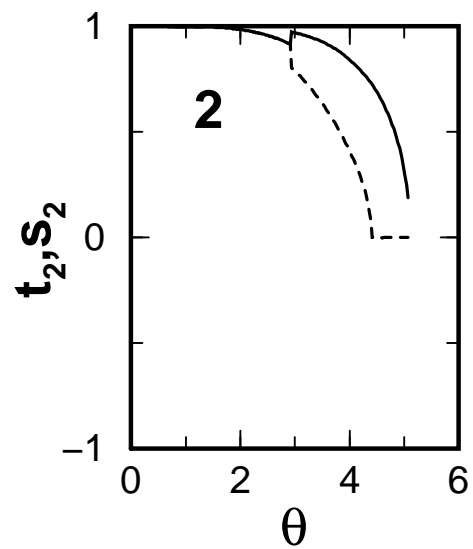
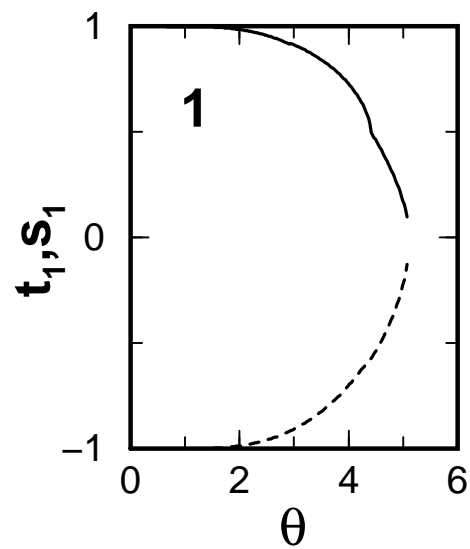
**Figure 7.**  $p$ - $T$  phase diagram of BCCD near the  $k = 1/4$ -phase. Solid lines: boundaries of the fourfold phase; dot-dashed lines:  $T_S$ -anomaly.  $\bullet$ : neutron scattering measurements [19];  $*$ : X-ray diffractometry [15]. a) Undisturbed sample (data from reference [18]). At ambient pressure,  $T_S$  coincides with the upper phase boundary. b) Sample for which X-ray induced defects are (schematically) taken into account. The temperature decrease is larger for  $T_S$  than for the phase boundaries. X-ray measurements at  $*$  should establish the structure above  $T_S$  even at ambient pressure.

**Figure 8.** Fourfold phase of BCCD: amplitudes  $Q_\ell^\tau$  and  $Q_\ell^\sigma$  of the  $\tau$ - and  $\sigma$ -SALMs as determined by the corresponding decompositions of neutron [19] (left hand side) and X-ray [15] (right hand side) data. In a Fourier series expansion only first and third (solid and dashed lines respectively) order harmonics in sine (cosine) are present in the spatial modulation of  $Q_\ell^\tau$  ( $Q_\ell^\sigma$ ). The neutron scattering results [19] show a much stronger third harmonic in the  $\sigma$ -SALM-profile than the X-ray diffraction measurements [15].

Neubert/Pleimling/Siems: FIGURE 1

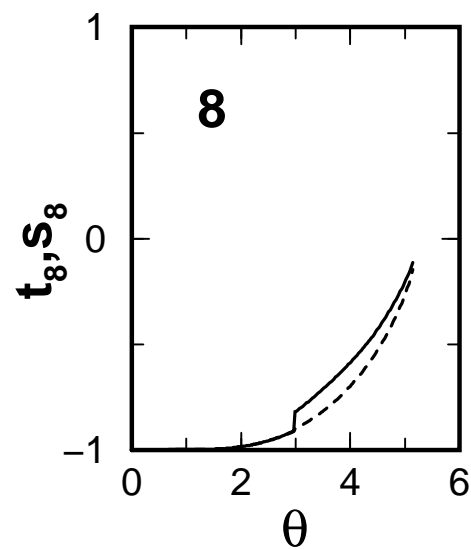
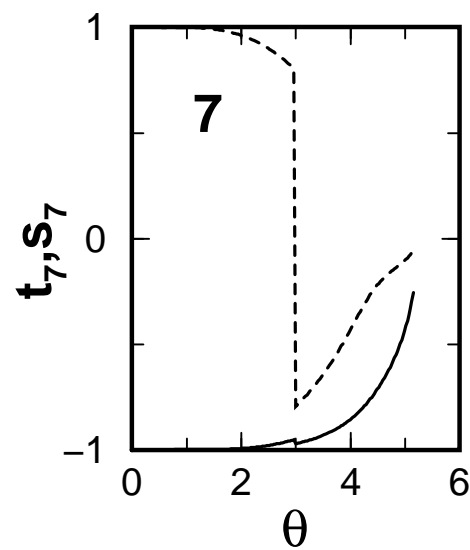
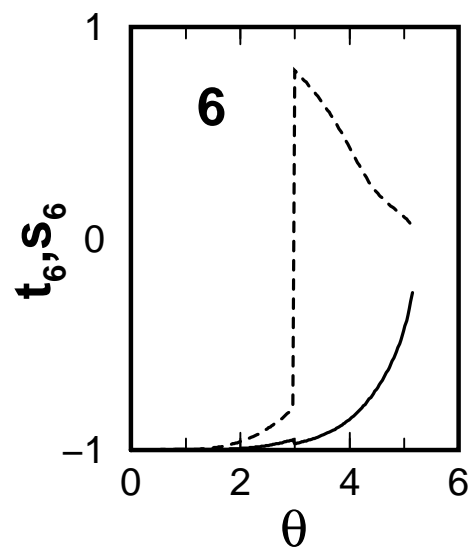
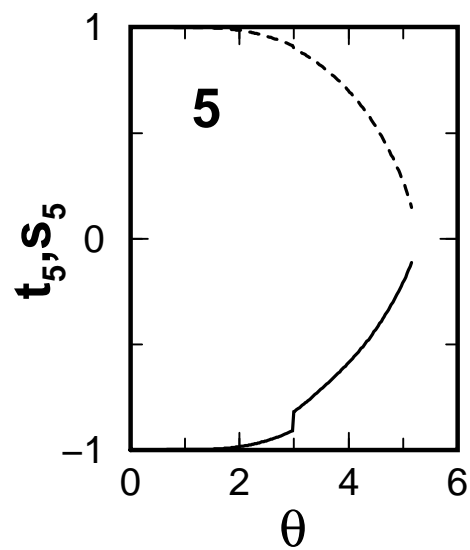
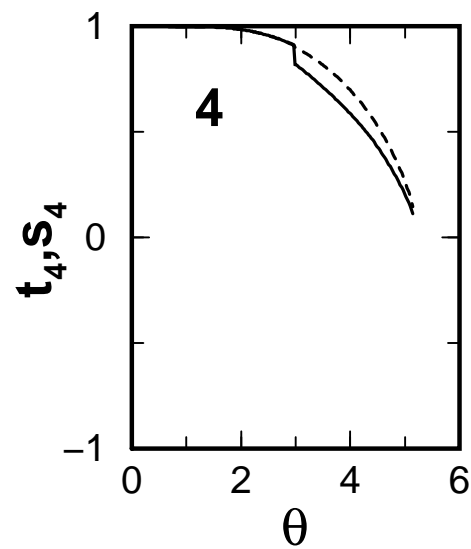
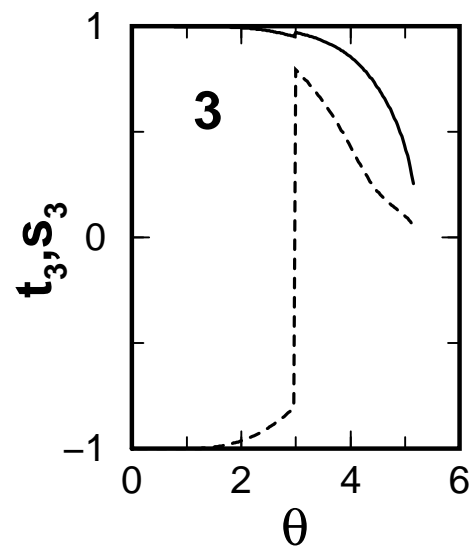
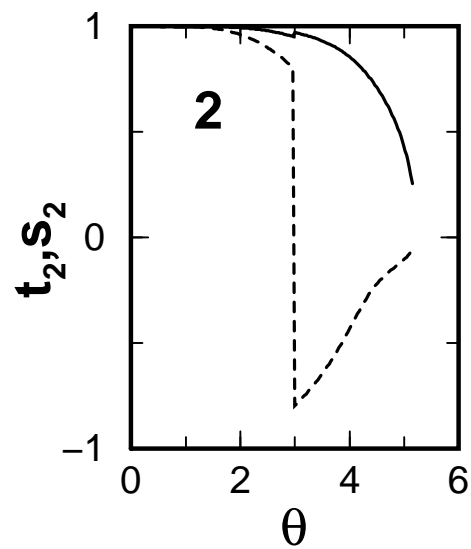
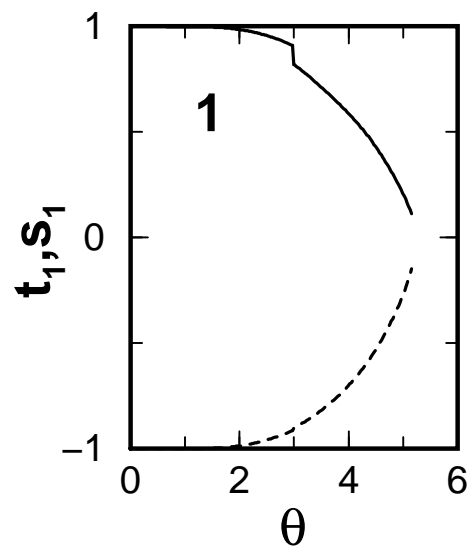


Neubert/Pleimling/Siems: FIGURE 2A

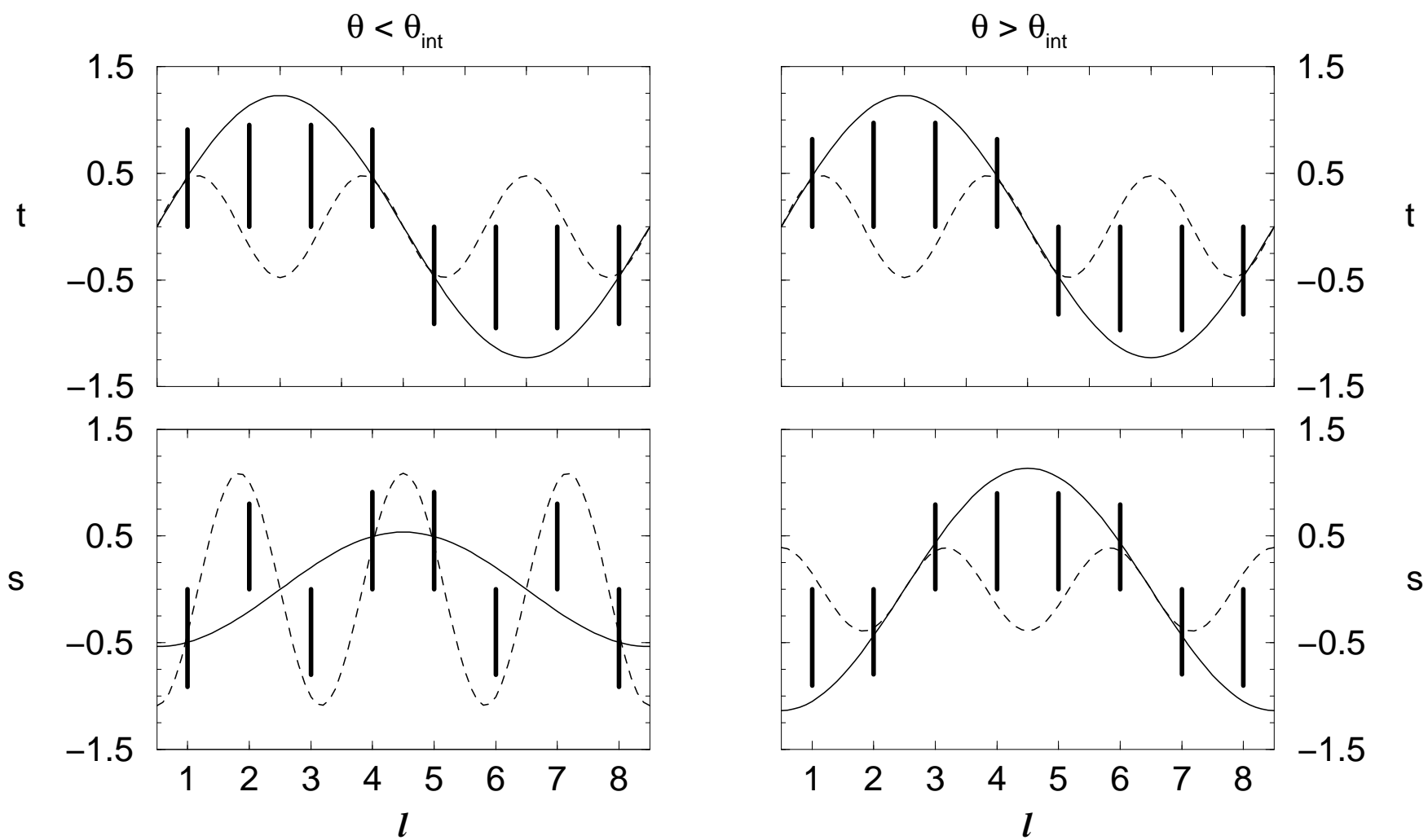




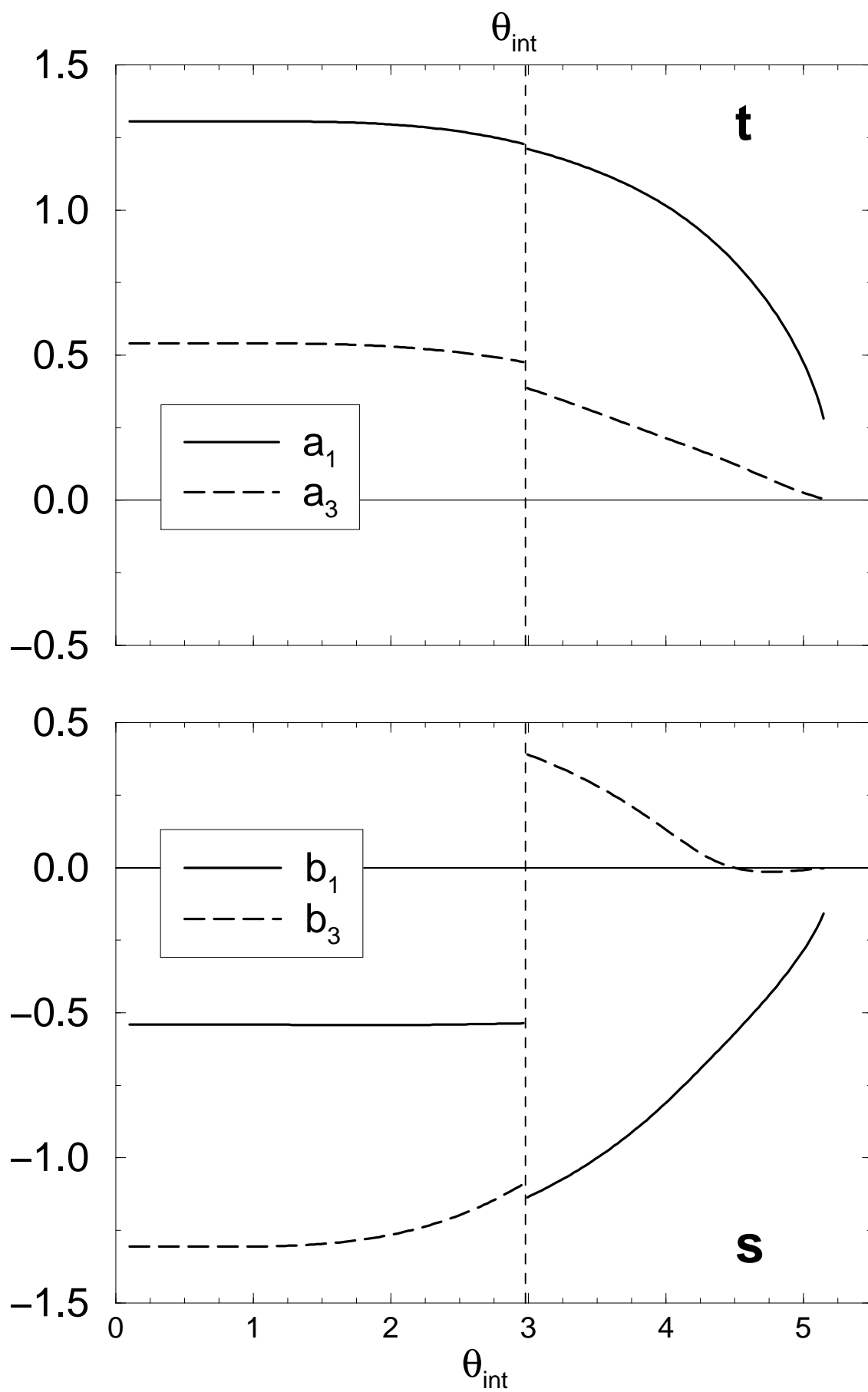
Neubert/Pleimling/Siems: FIGURE 2B



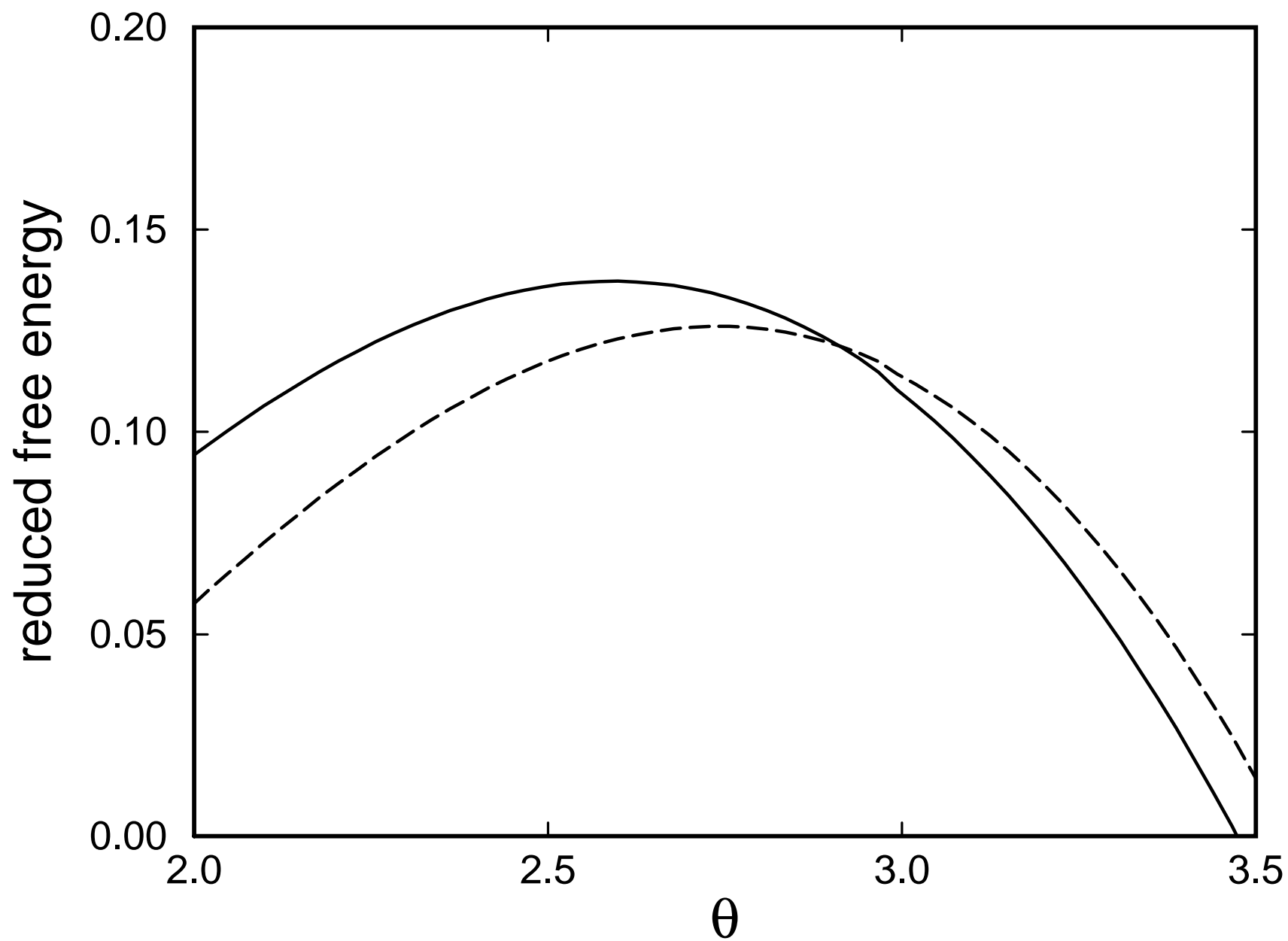
Neubert/Pleimling/Siems: FIGURE 3



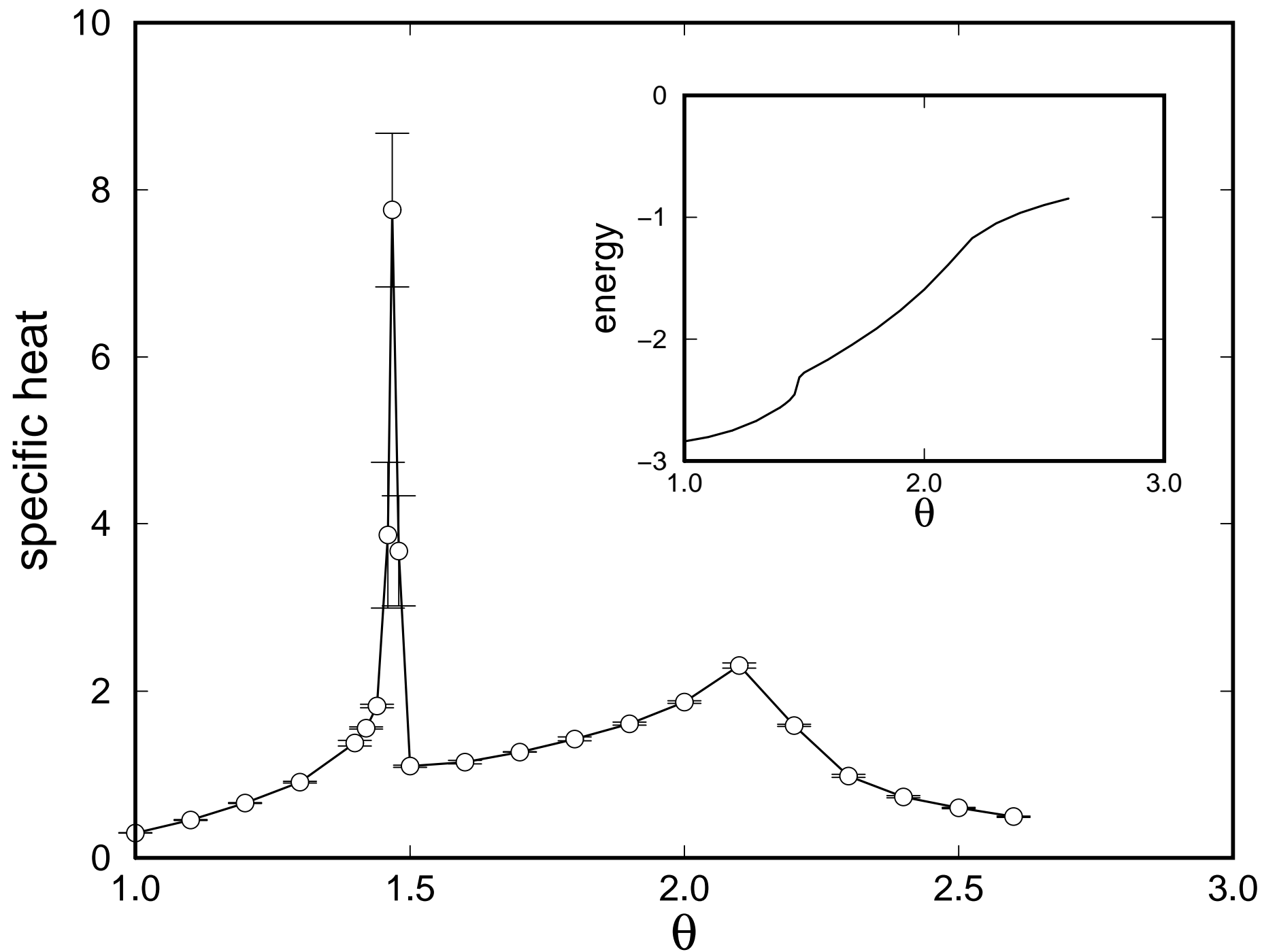
Neubert/Pleimling/Siems: FIGURE 4



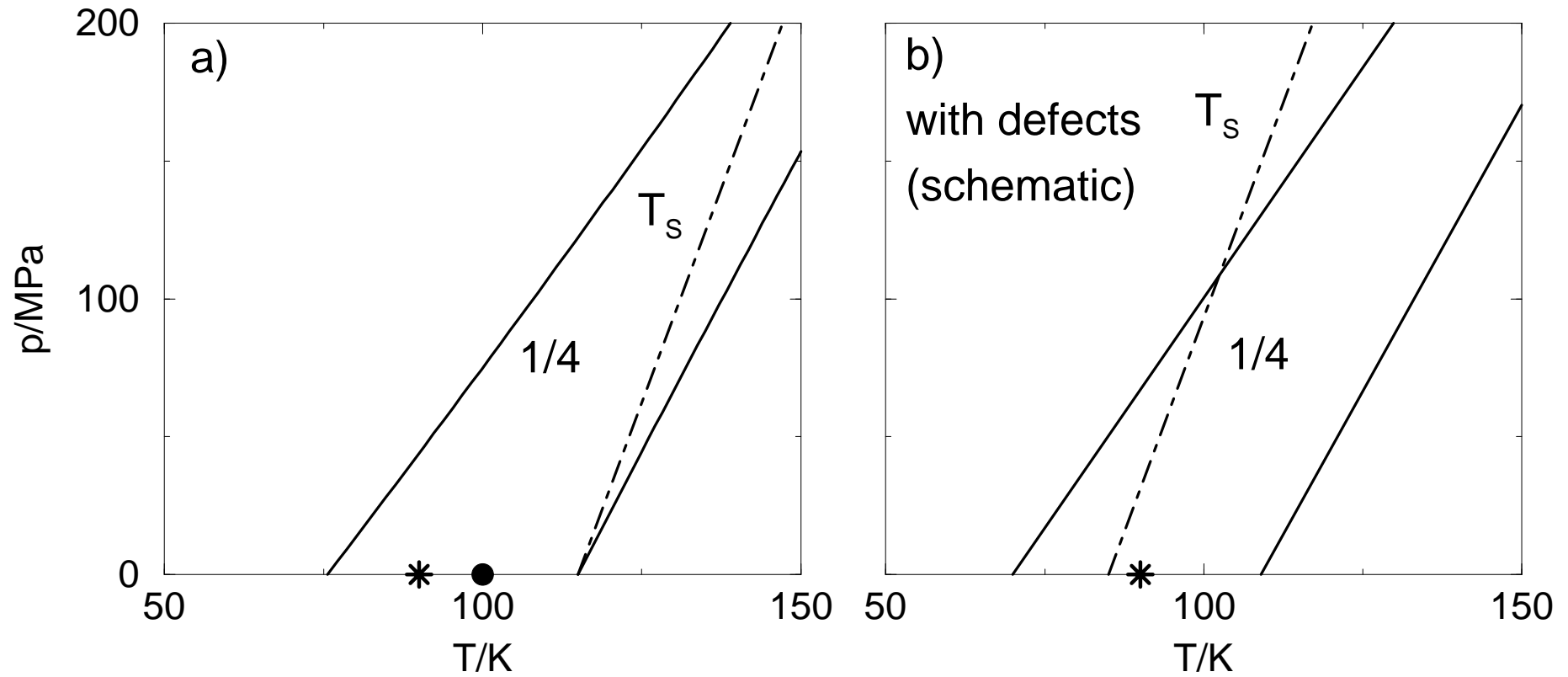
Neubert/Pleimling/Siems: FIGURE 5



Neubert/Pleimling/Siems: FIGURE 6



**Neubert/Pleimling/Siems: FIGURE 7**



Neubert/Pleimling/Siems: **FIGURE 8**

